

## SUPPLEMENTARY FIGURE LEGENDS

### Supplementary Figure 1

#### Quantification of siRNA knock-down efficiency.

Immunofluorescence staining against CSPP/CSPP-L (red) and  $\gamma$ -tubulin (green) of HeLa cells 72h post transfection with either GFP or CSPP/CSPP-L mRNA (SMARTpool) targeting siRNA (A) or a single siRNA CSPP/CSPP-L targeting siRNA. Line graphs show fluorescence signal intensities of CSPP/CSPP-L (red) and  $\gamma$ -tubulin (green) detection along a line crossing peak intensities of  $\gamma$ -tubulin. Images were taken with identical settings and are displayed with identical LUT scales. K

### Supplementary Figure 2

#### CSPP-L is expressed in human B cells and localizes to centrosomes and the midbody.

Immunofluorescence staining of the B cell leukemia cell line Reh for CSPP-L (green) and  $\gamma$ -tubulin (red). CSPP-L co-localizes with  $\gamma$ -tubulin at centrosomes and at the midbody. Reh cells were fixed and stained as described in materials and methods, except staining was performed in 4ml tubes. For microscopy cells were sedimented and carefully re-suspended in Vecta Shield (VECTOR LABORATORIES, INC., Burlingame, CA, USA), mounted on slides with No1.5 cover slips and sealed with clear nail polish.

### Supplementary Figure 3

#### Subcellular localization of CSPP-egfp, CSPP-L-egfp fusion proteins and truncation mutants in serum starved hTERT-RPE1 cells.

(A) Live cell imaging of serum starved hTERT-RPE1 cells transiently transfected with either CSPP-L-egfp (left) or CSPP-egfp (right) expression plasmids show both EGFP-fusion proteins (green) specifically enriched at basal bodies and cilia axonemes. (B) The CSPP-L specific N-terminal 294 amino acids show cytoplasmic and nuclear localization and enrich along stress fibres and at the centrosome (see (C)) The common central coiled-coil domains (amino acids 295 to 709 in CSPP-L) have been described earlier to decorate microtubules and enrich specifically at cilia and the basal body, whereas the C-terminal shows cytoplasmic and nuclear staining and enriches at centrosomes in agreement with earlier results (Patzke *et al.*, 2006). (C) Immunofluorescence staining for actin (red) and acetylated tubulin (blue) of formalin fixed serum starved hTERT-RPE1 cells transiently expressing the CSPP-L specific N-terminal domain (green) confirms its affinity for actin fibres and centrosomes as suggested by the live cell imaging data.

#### **Supplementary Figure 4**

##### **CSPP1 gene expression in whole mouse embryo sections and CSPP/CSPP-L protein expression in adult mouse trachea epithelia cells.**

(A) *CSPP1* gene expression determined by non-radioactive in situ hybridization on serial tissue sections of a whole C57BL/6 mouse embryo at stage E14.5. Data obtained from GenePaint consortium ([www.genepaint.org](http://www.genepaint.org)), GenePaint Set ID: EH3844, CSPP1. *CSPP1* is highly expressed in various ciliated tissues during mouse development. (B) Z-Projection of optical sections of immunofluorescence images of ciliated trachea epithelia cells isolated from adult BALB/C nu/nu mice stained for CSPP/CSPP-L proteins (a-CSPP/CSPP-L, red) and IFT88 as marker of motile cilia (a-IFT88, green). The right panel displays a 3-D model of the apical cell membrane showing the enrichment of CSPP/CSPP-L proteins at basal body containing layer.

#### **Supplementary Figure 5**

##### **Efficacy of single CSPP/CSPP-L and CSPP-L targeting siRNAs and effects of CSPP/CSPP-L depletion on cell cycle progression.**

(A) HEK293T cells were transiently transfected with expression plasmids for CSPP-myc or CSPP-L-myc proteins alone or together with the single siRNAs designed to target either both or solely the large CSPP-L. The siRNA designed to target both CSPP isoforms efficiently competes with SV40 promoter driven expression of CSPP-myc and CSPP-L-myc, whereas the CSPP-L specific siRNA only competes with CSPP-L-myc expression. (B) Asynchronously growing hTERT-RPE1-hTERT cells were transfected with either control or CSPP/CSPP-L targeting siRNA and analyzed 72h post-transfection for cell cycle phase distribution by DNA staining and flow-cytometry as described in (Mikule *et al.*, 2007). DNA histograms of CSPP/CSPP-L siRNA transfectants showed a decreased G<sub>2</sub>/M population indicating (representative data shown). (C) To test if CSPP/CSPP-L transfection interfered with S-phase entry/progression cells were pulse labeled with BrdU 30 min prior analysis and BrdU and the number of BrdU incorporating cells assessed by immunofluorescence. CSPP/CSPP-L siRNA transfectants showed a two to three fold decrease in DNA synthesizing cells. Error bars indicate standard deviation of three experiments. The results in (B) and (C) are indicative for a G<sub>0</sub>/G<sub>1</sub> phase arrest.

#### **Supplementary Figure 6**

##### **CSPP proteins are required for stabilization of NPHP8 but not NPHP4 at the basal body.**

(A) Immunofluorescence images of serum starved hTERT-RPE1 cells transfected with siRNAs targeting GFP (control, upper panel) or CSPP/CSPP-L (SMARTpool, lower panel) and stained for the centriole and ciliary marker acetylated tubulin (blue), NPHP8 (red) and NPHP4 (green). Cilia defective CSPP/CSPP-L siRNA transfectants show diminished levels of NPHP8 but not NPHP4 at the ciliary base. (B) Conversely, elongated primary cilia in NPHP8 siRNA transfectants show ciliary localization of CSPP-L (green) and unaltered levels of NPHP4 (red) at the ciliary base.

### **Supplementary figure 7**

#### **Schematic presentation of a putative CSPP containing NPHP protein network.**

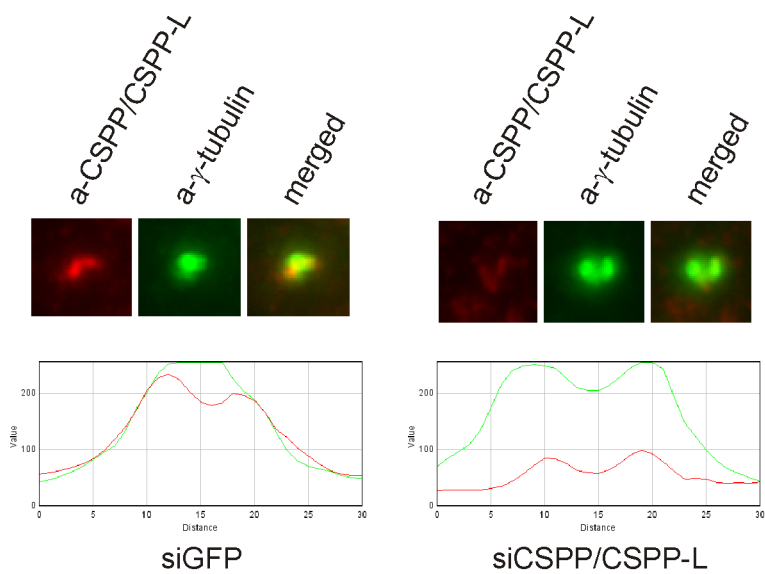
NPHP1, NPHP4 and NPHP8 form a core axis. This axis can affect cytoskeletal organization and thereby planar cell polarity either through direct interactions (NPHP1 – actin cytoskeleton, NPHP8 – microtubule/actin cytoskeleton via CSPP/CSPP-L) or indirectly via feeding into WNT or Hh signaling pathways. It is believed that malfunction of these pathways may disrupt normal tissue architecture and result renal cyst formation. NPHP9/NEK8 has not been placed in this scheme since its phosphorylation targets at the basal body/cilium have yet not been identified. Two ciliogenesis regulating arms converge at NPHP8. Firstly, via binding to RPGR, which interacts with NPHP6 that controls ciliogenesis by recruitment of Rab8 under control of CEP110 and secondly, via CSPP/CSPP-L that possibly controls ciliogenesis via its interactions to cytoskeleton organizing proteins. Our findings suggest that NPHP8 might be part of CSPP-L containing functional unit capable to interact with NPHP4. CSPP-L is crucial to promote the recruitment or maintenance of NPHP8 at the basal body. NPHP8 than might act antagonistically on CSPP-L to regulate cilia length since either depletion of NPHP8 or over-expression of CSPP-L results in a prolonged cilia phenotype.

### **Supplementary Figure 8**

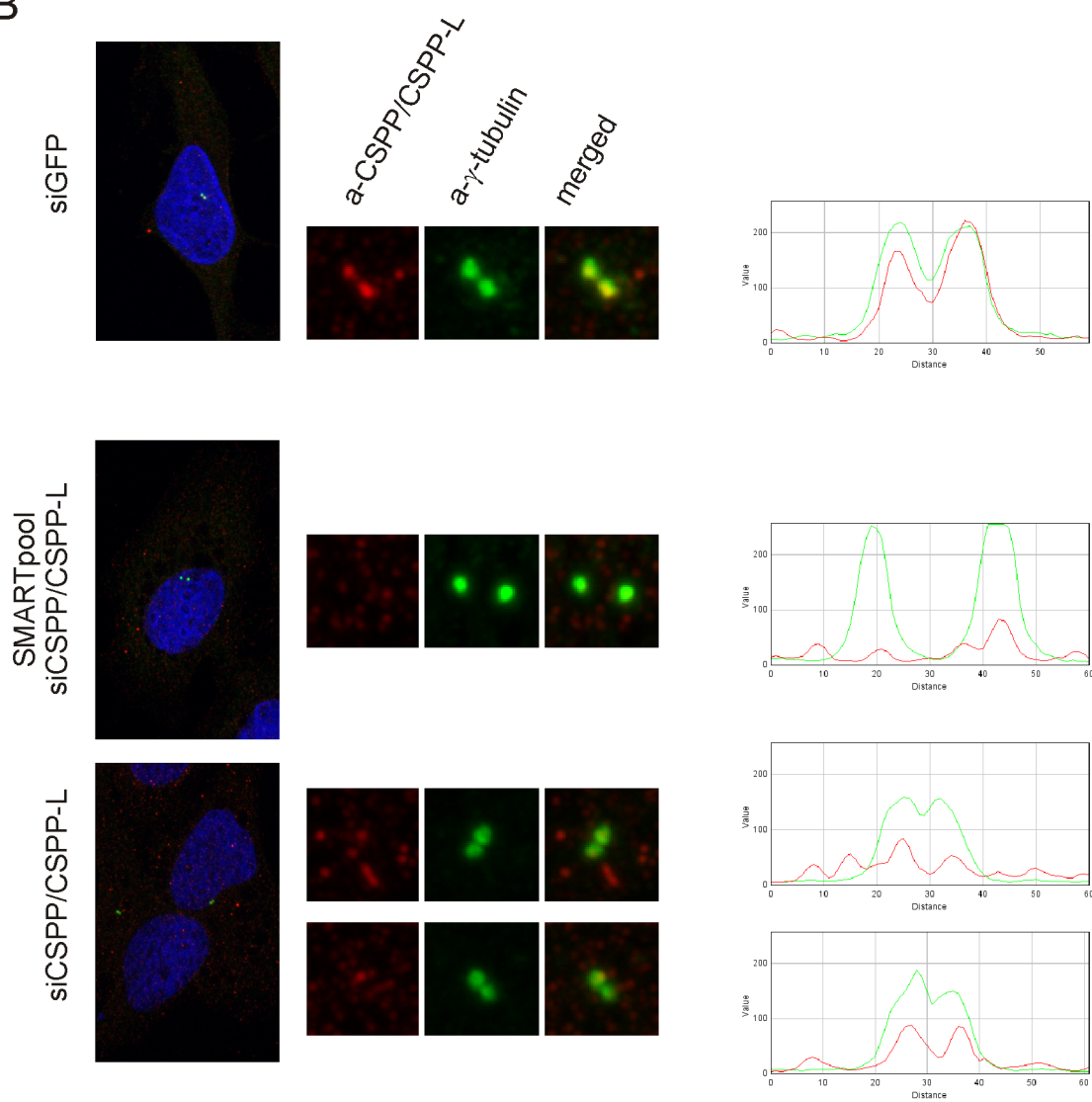
**Alignment of protein sequences of human CSPP-L (GenBank: Q1MSJ5) and a predicted protein in the choanoflagellate *Monosiga brevicollis* (GenBank: XP\_001748901).**

# Supplementary figure 1

A



B

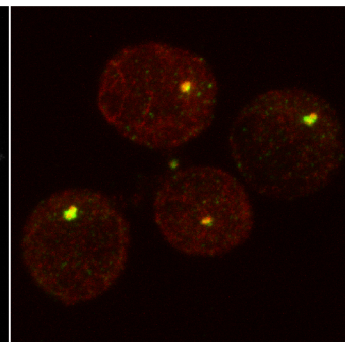
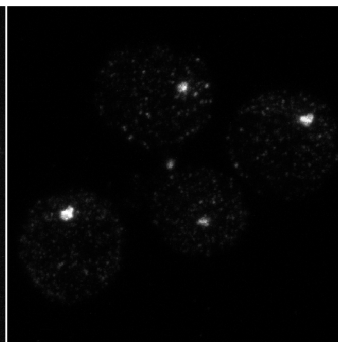
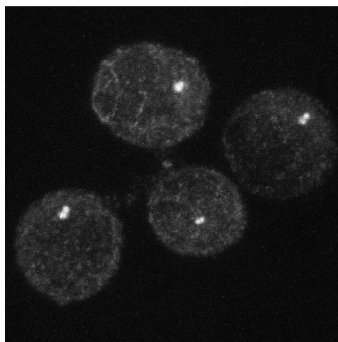
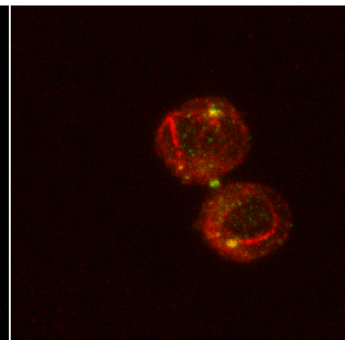
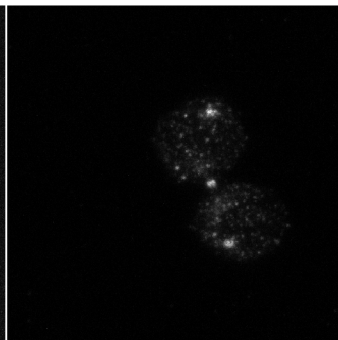
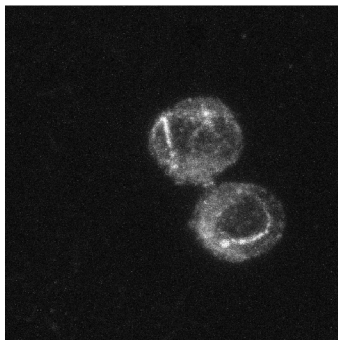


# Supplementary figure 2

a- $\gamma$ -tubulin

a-CSPP-L

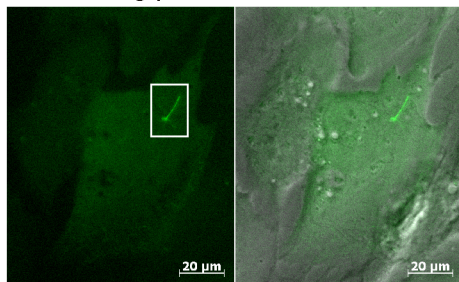
merged



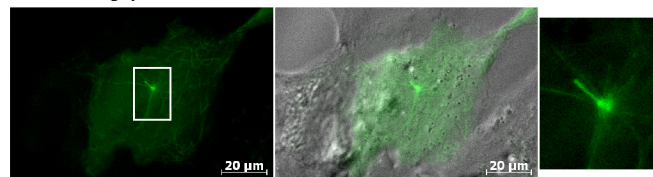
# Supplementary figure 3

A

CSPP-L-egfp

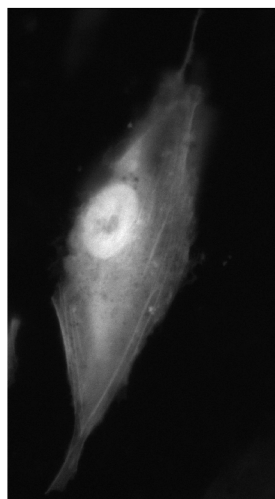


CSPP-egfp

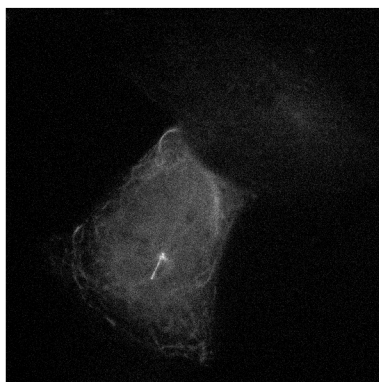


B

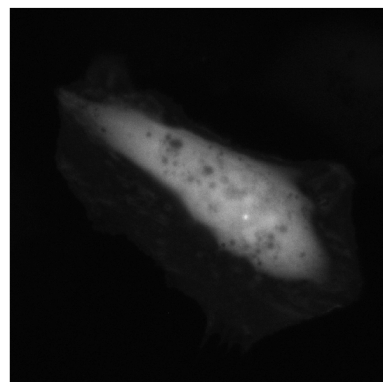
CSPP-L-egfp $\Delta$ 295-1221



CSPP-egfp $\Delta$ 504-876



CSPP-egfp $\Delta$ 1-498



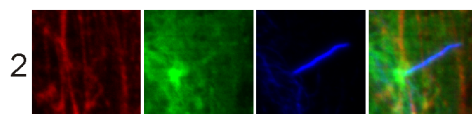
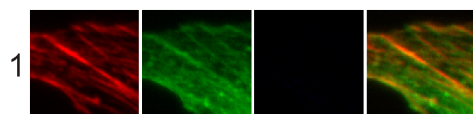
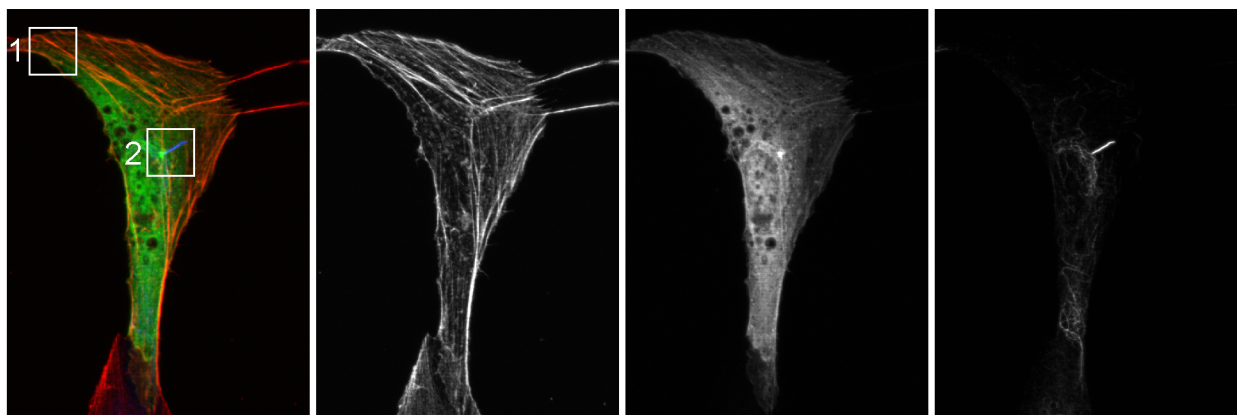
C

merged

actin

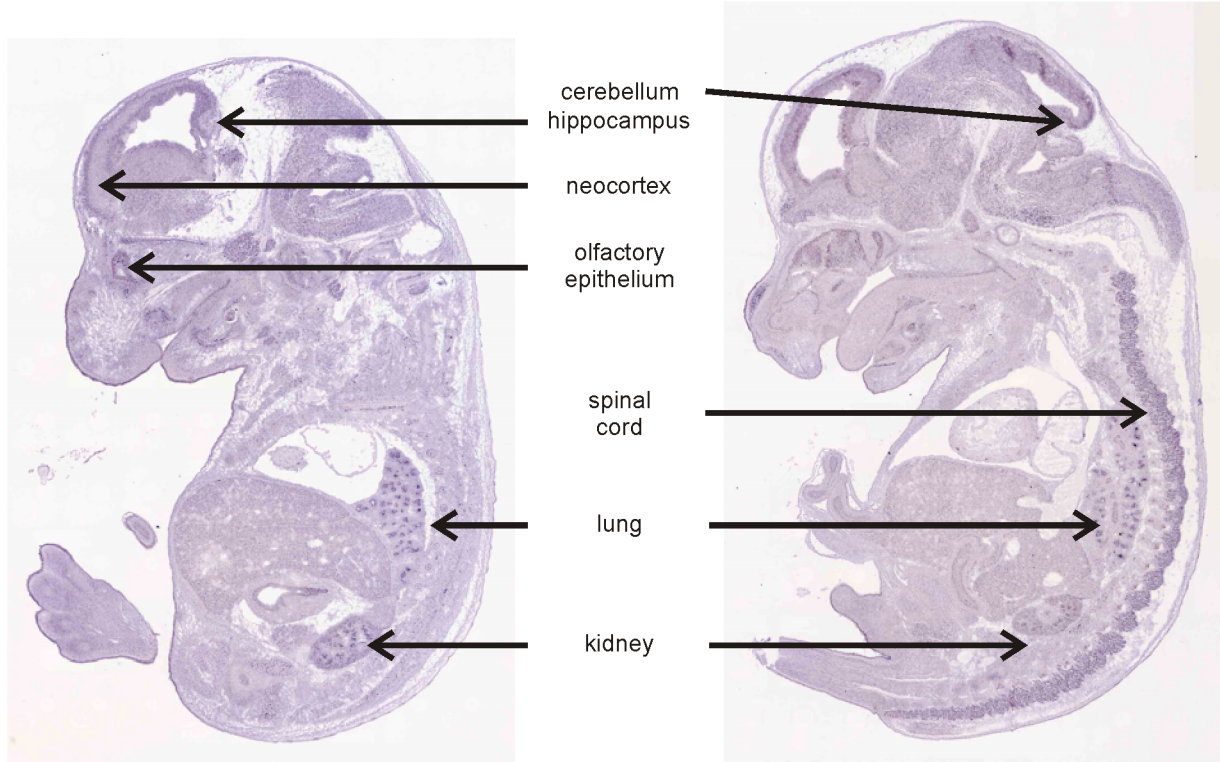
CSPP-L-egfp $\Delta$ 295-1221

acetylated tubulin



# Supplementary figure 4

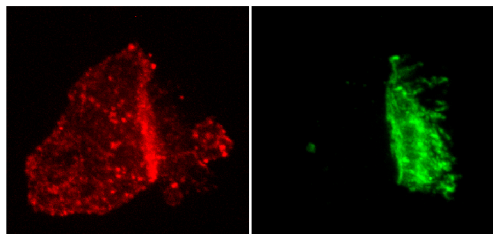
A



B

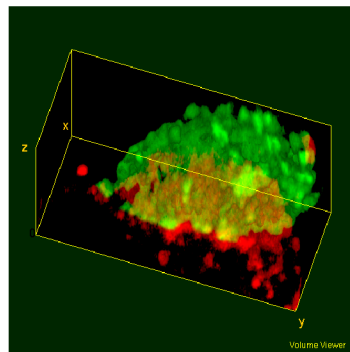
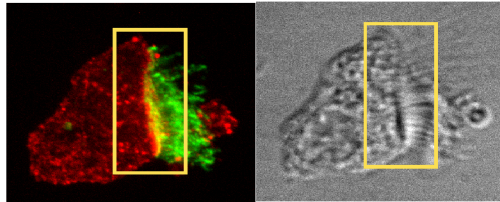
a-CSPP/CSPP-L

a-IFT88



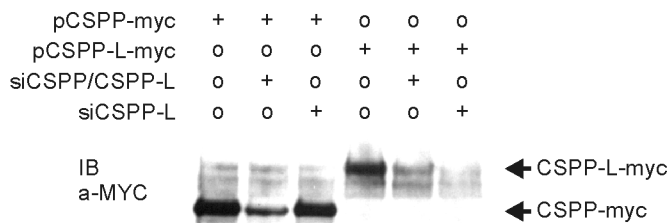
merged

DIC

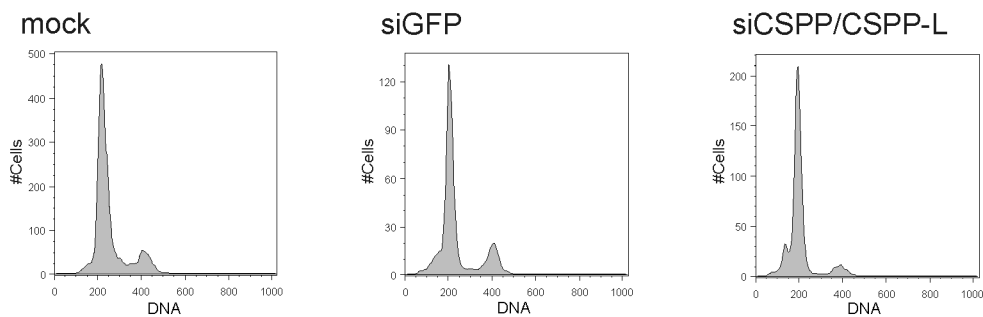


# Supplementary figure 5

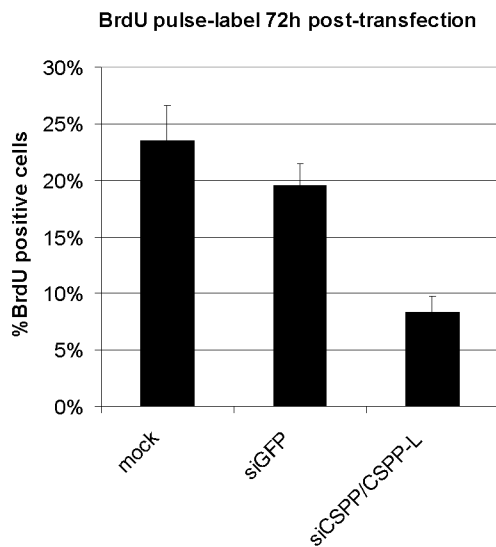
A



B



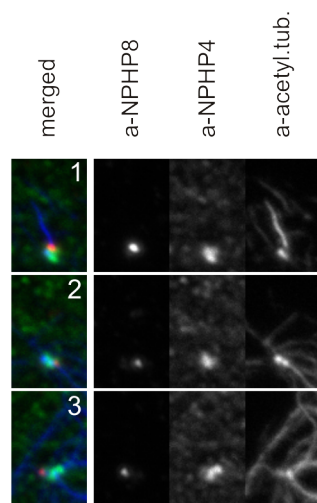
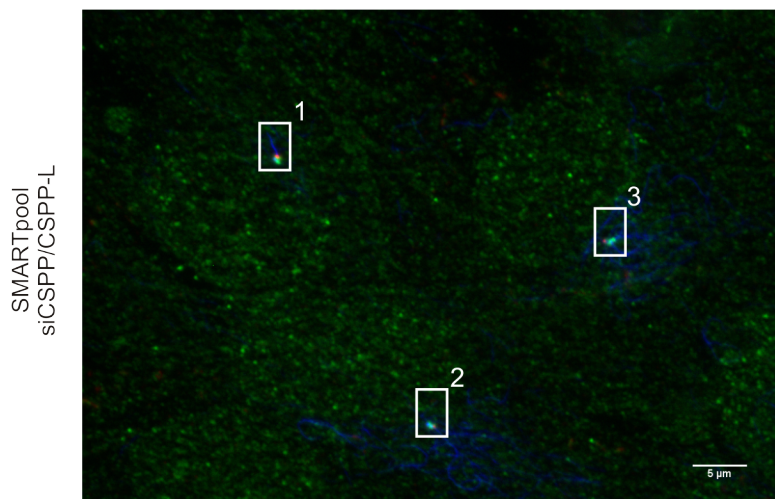
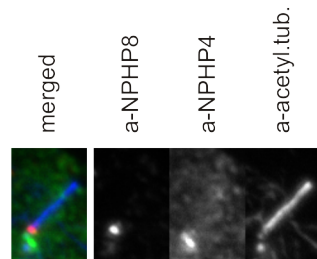
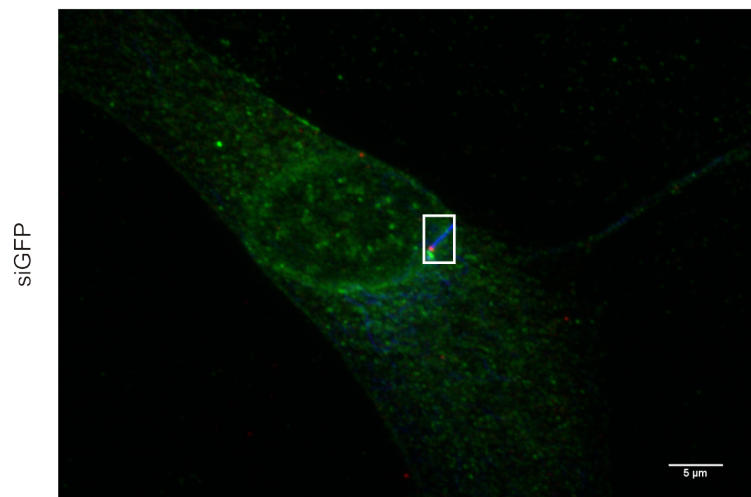
C



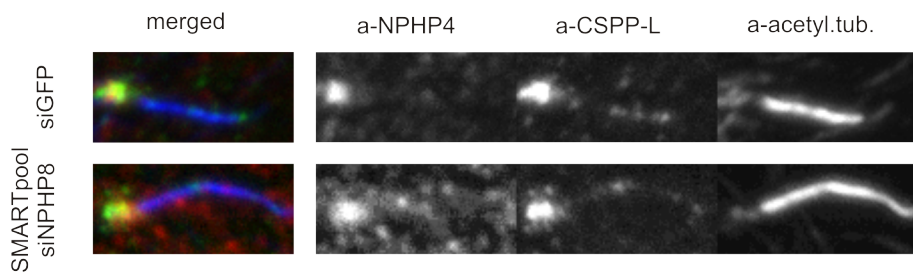


# Supplementary figure 6

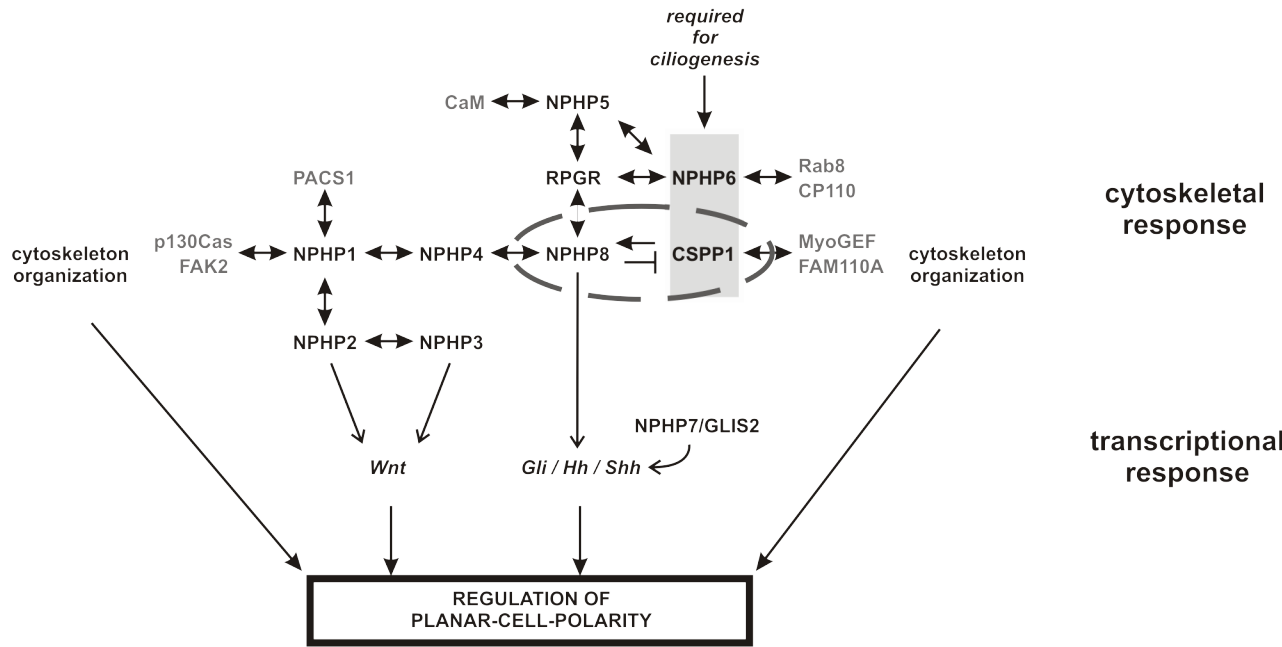
A



B



# Supplementary figure 7



# Supplementary figure 8

